



Published in final edited form as:

Nat Biotechnol. 2008 June ; 26(6): 702–708. doi:10.1038/nbt1409.

Heritable Targeted Gene Disruption in Zebrafish Using Designed Zinc Finger Nucleases

Yannick Doyon^{2,4}, Jasmine M McCammon^{1,4}, Jeffrey C Miller², Farhoud Farajji², Catherine Ngo², George E Katibah², Rainier Amora², Toby D Hocking², Lei Zhang², Edward J Rebar², Philip D Gregory², Fyodor D Urnov^{1,2}, and Sharon L Amacher^{1,3}

¹ Department of Molecular and Cell Biology and Center for Integrative Genomics, University of California, Berkeley, CA 94720-3200, USA

² Sangamo BioSciences, Inc., Pt. Richmond Tech Center, 501 Canal Blvd., Suite A100, Richmond, CA

Abstract

We describe here the use of zinc finger nucleases (ZFNs) for somatic and germline disruption of genes in zebrafish (*Danio rerio*), where targeted mutagenesis was previously intractable. ZFNs induce a targeted double-strand break in the genome that is repaired to generate small insertions and deletions. We designed ZFNs targeting the zebrafish *golden* and *no tail/Brachyury* genes. In both cases, injection of ZFN-encoding mRNA into 1-cell embryos yielded a high percentage of animals carrying distinct mutations at the ZFN-specified position and exhibiting expected loss-of-function phenotypes. Disrupted *ntl* alleles were transmitted from ZFN mRNA-injected founder animals in over half the adults tested at frequencies averaging 20%. The frequency and precision of gene disruption events observed, in combination with the ability to design ZFNs against any locus, open fundamentally novel avenues of experimentation, and suggest that ZFN technology may be widely applied to many organisms that allow mRNA delivery into the fertilized egg.

The zebrafish has proven to be an excellent model for vertebrate development and disease 1 due to its rapid development, transparent embryos, and its relatively facile forward genetics. Techniques for reverse genetic approaches in zebrafish, however, are limited to mRNA knockdown strategies using modified antisense oligomers (morpholinos) 2 and TILLING for point mutations in a locus of interest. Both strategies have shortcomings and are limited in scope: morpholinos are active for only the first few days of development, hence their transient effect fails to impact on juvenile or adult phenotypes, while TILLING is both time-consuming and less effective for intron-rich genes with small exons because the chances of obtaining null or hypomorphic alleles are reduced 3. Conventional “gene targeting,” a

Users may view, print, copy, and download text and data-mine the content in such documents, for the purposes of academic research, subject always to the full Conditions of use:http://www.nature.com/authors/editorial_policies/license.html#terms

³To whom correspondence should be addressed: amacher@berkeley.edu. Correspondence regarding, and requests for, zinc finger nuclease reagents described in the paper should be directed to furnov@sangamo.com.

⁴These authors contributed equally to this work.

Author Contributions

F.D.U. and S.L.A. conceived the project; Y.D., J.M.M., J.C.M., L.Z., E.J.R., F.D.U. and S.L.A. designed experiments; Y.D., J.M.M., F.F., C.N., G.E.K., R.A., T.D.H. and S.L.A. performed experiments; Y.D., J.M.M., P.D.G., F.D.U. and S.L.A. wrote the manuscript.

powerful technique for gene disruption in mouse embryonic stem cells 4, often requires positive-negative selection with cytotoxic drugs 5, which is inapplicable in the context of a vertebrate embryo.

The resistance of the genome in most metazoa to targeted sequence alteration 5 has recently been overcome through the use of zinc finger nucleases (ZFNs). Initially developed to cleave DNA *in vitro* 6, ZFNs are a fusion between the cleavage domain of the type IIS restriction enzyme, FokI, and a DNA recognition domain containing 3 or more C₂H₂ zinc finger motifs. The heterodimerization at a particular position in the DNA of two individual ZFNs in precise orientation and spacing leads to a double-strand break (DSB) in the DNA 7. DSB repair pathways operate in all eukarya, and include non-homologous end-joining (NHEJ, the direct ligation of the two DNA ends, frequently with loss or gain of small amounts of DNA sequence), as well as homology-directed repair 8. Importantly, Carroll and colleagues 9 exploited NHEJ-based repair of a ZFN-induced DSB to disrupt a gene in *Drosophila* and an intergenic region in *C. elegans* 10, thus establishing the potential of this technology in reverse genetic applications, recently expanded to mammalian tissue culture cells 11. Here, using *golden/slc24a5 (gol)* and *no tail/Brachyury (ntl)* as test loci, we investigated the feasibility of using designed ZFNs for reverse-genetic applications in zebrafish.

The *gol* pigment locus encodes a transmembrane protein, Slc24a5 12, and was chosen for an initial test of ZFN-driven editing because the lack of embryonic pigmentation caused by homozygous viable *gol* mutations make scoring for ZFN activity by loss-of-function straightforward 13. The C₂H₂ zinc finger is a versatile DNA binding motif capable of recognizing a broad range of sequences 14, and efforts over the past 14 years have yielded a large number of zinc fingers aimed at recognizing investigator-specified DNA triplets (see Supplementary Information online). As a consequence, simple *in silico* analysis can illuminate a high number of potential zinc finger proteins (ZFPs) for any given target gene. We describe here an experimentally straightforward two-step approach to identify those particular ZFPs that will yield robust ZFNs for *in vivo* gene disruption, and its application to the zebrafish *gol* and *ntl* genes.

We analyzed *in silico* the cDNA sequence of the *gol* gene and assembled a panel of 4-finger ZFPs (see Materials and Methods, Supplementary Information, and Supplementary Fig. 1 online) directed against a range of distinct positions in the *gol* locus (Supplementary Table 1 online). To limit the number of ZFN pairs to be tested *in vivo*, the affinity of the ZFPs for their target sequence was measured using an ELISA assay (Supplementary Fig. 2 online). Next, to determine which of these ZFPs will form pairs most likely to be active in zebrafish gene disruption, we developed a budding yeast-based system to rapidly measure ZFN activity (Fig. 1A–B; Supplementary Fig. 3 online; a detailed description is provided in Supplementary Information online).

In building this system, we made use of the well-established fact that while NHEJ operates relatively inefficiently in budding yeast, a DSB induced between two short direct repeats spaced by a heterologous sequence of up to 25 kb leads to resection of the entire intervening DNA, and the restoration of chromosome integrity via the single-strand annealing of the two

repeats 15. We disabled the open reading frame for a secreted form of alpha-galactosidase (encoded by the *MEL1* gene) with the *gol* sequence and placed this construct into a specific position of the budding yeast genome. Experiments using a control construct, in which the DSB between the direct repeats was induced by the well-studied yeast endonuclease, HO, validated the dynamic range and low background of the system in reporting the efficiency of DSB induction by the nuclease (Fig. 1C–D). We then screened the panel of *gol*-targeting ZFNs for DNA cleavage activity in a budding yeast reporter strain carrying their target sequence (Fig. 1A). This analysis identified active ZFN pairs directed against exons 4, 8, and 9 of the *gol* gene (Fig. 2A) – we focused on the exon 4 and 9-targeting ZFNs in subsequent experiments (Fig. 2B, Supplementary Fig. 4 online).

Following screening in budding yeast, the ZFNs identified as active in that system were tested for native gene disruption activity at their intended target locus in zebrafish: the ZFN expression constructs were transcribed and capped *in vitro*, and the resulting mRNAs were injected into 1-cell zebrafish embryos heterozygous for the *gol^{bl}* mutation 12. For the majority of our experiments we used ZFNs carrying obligate-heterodimer forms of the FokI endonuclease domain 16; these inhibit ZFN homodimerization and thus improve specificity by limiting cleavage at off-target sites recognized by ZFN homodimers 16. At 2 days post fertilization (dpf), *gol^{bl}* heterozygotes normally have dark eye pigmentation (Fig. 2C, upper left); however, we detected clones of unpigmented cells in the eye, potentially representing loss of *gol* function on the non-*gol^{bl}* chromosome, in up to 32% of ZFN-injected, but not in control, embryos (Table 1 and Fig. 2C). A clear positive correlation was observed between extent of mosaicism and amount of ZFN mRNA injected (Table 1). At the highest doses of ZFNs, over 30% of injected embryos exhibited pigmentation mosaicism in the eye (Table 1). Also at the highest ZFN doses, a small fraction of ZFN-injected embryos exhibited mild to moderate developmental defects, such as a bent body axis or mild head necrosis. However, even at the highest concentrations tested, the majority of embryos showing pigment mosaicism were indistinguishable from wild-type embryos (69–90% depending on the ZFN pair tested) (Table 1).

To investigate whether these phenotypes were the consequence of somatic loss-of-function mutations resulting from repair of ZFN-induced DSBs by NHEJ, we genotyped the *gol* locus in injected embryos. We used PCR to amplify a 312 bp region including the ZFN target site, with total genomic DNA from individual fish with *gol* clones serving as the input for each PCR reaction. Consistent with the phenotypes observed above, we found a broad range of loss-of-function alleles in the genomes of ZFN-injected animals, but not in controls (data not shown). These included deletions ranging in size from 7 to 65 bp and insertions of 4 to 12 bp (Fig. 2D). Taken together, these experiments demonstrated that a single injection of ZFN-encoding mRNA into an early zebrafish embryo can result in the efficient mutation of the locus targeted by the ZFNs to yield alleles that confer loss-of-function phenotypes.

To confirm the generality of the observations above, we next targeted the *no tail/Brachyury* (*ntl*) gene, a major regulator of early embryogenesis. The choice of target gene was in large part inspired by the fact that the study of early development is a major direction of biological investigation in zebrafish as a model system. The *ntl* gene encodes an essential T-box transcription factor required for proper mesoderm formation; zebrafish embryos

homozygous for a null *ntl* mutation lack a notochord and a tail 17. To test whether ZFNs can induce somatic mutations in the *ntl* gene, we followed the same scheme described for the *gol*-targeting ZFNs (ZFN design, ELISA *in vitro* binding assay, and *in vivo* yeast-based activity assay) (Fig. 3A; Supplementary Table 2 and Fig. 5 online). For these experiments, we focused our design efforts on exon 2, the location of a well-studied null allele of the gene (Fig. 3B).

Using lead proteins (Supplementary Fig. 6 online) identified in the yeast-based assay (Fig. 3A) for our initial effort in *ntl* disruption, we injected mRNA encoding high-fidelity, obligate-heterodimer 16 ZFNs into 1-cell embryos from a cross between wild-type and *ntl*^{b195} heterozygous fish. Since half the injected embryos carry the *ntl*^{b195} null allele, we hypothesized that these embryos would reveal ZFN-driven mutations of the wild-type allele on the other chromosome. Strikingly, we observed that 16–27% of injected embryos displayed a *ntl*-like phenotype (Fig. 3D), either mimicking the null phenotype 17 (Fig. 3C) or a less severe phenotype typical of a hypomorphic allele, *ntl*^{b487} (Supplementary Fig. 7 online). We noted that even high ZFN mRNA doses were well-tolerated by the embryos (Fig. 3D).

We genotyped individual *ntl*-like embryos at the ZFN target stretch using a rapid assay based on a mismatch-sensitive endonuclease 16 that allows one to measure the fraction of chromatids carrying mutations relative to the wild-type sequence. This analysis showed that the fraction of mutated chromatids ranged from 3 to 17% in the majority of embryos (Supplementary Fig. 8 online). To further analyze the types of mutations induced, we sequenced a 226 bp region surrounding the DSB site from ZFN-injected embryos, and observed a broad range of deletions and insertions precisely at the targeted locus (Fig. 3E). The mutant sequences shown in Fig. 3E appear to represent alleles generated by NHEJ-induced repair of the ZFN-cleaved chromatid, because chromatids bearing the ~1.5 Kb *ntl*^{b195} insertion (see Fig. 3B) are too large to be amplified and analyzed.

Given our published data on the feasibility of generating single-step biallelic genome editing events using ZFNs in human cells 18, we analyzed whether wild-type embryos injected with high-fidelity *ntl*-targeting ZFNs displayed *ntl* mutant phenotypes. In these experiments, we found that juvenile and adult fish had posterior tail truncations (20% [3/15] and 21% [12/58] among stocks injected with 1 ng and 5 ng ZFN Pair 2, respectively, and 7.7% [4/52] among stocks injected with 5 ng ZFN Pair 3) (Fig. 4A). We sequenced the *ntl* locus surrounding the ZFN-cleavage site from a small posterior tissue sample from each of three tailless embryos and found that *ntl* mutant-bearing amplicons represent a substantial fraction of the total (Sample 1, 5/25 (20%) *ntl*-bearing chromatids, 2 different alleles; Sample 2, 3/30 (10%) *ntl*-bearing chromatids, 1 allele; Sample 3, 8/29 (28%) *ntl*-bearing chromatids, 4 different alleles) (Supplementary Fig. 9 online).

Interestingly, when *ntl*-targeting ZFNs carrying wild-type FokI cleavage domains were injected into wild-type embryos, a high frequency of embryos exhibiting a *ntl* phenotype were observed; sequencing a 226 bp region surrounding the DSB site revealed that each of 3 representative embryos carried between 64–81% disrupted *ntl* alleles (Table 2; Supplementary Fig. 10 online). Given that a single wild-type *ntl* allele is sufficient for a

normal phenotype, these data suggest that ZFNs can induce biallelic disruption of a target gene locus after mRNA injection into the 1-cell embryo.

To demonstrate that ZFNs can effectively induce mutations in the germline, wild-type embryos injected with *ntl*-targeting high-fidelity 16, obligate-heterodimer ZFNs were raised to sexual maturity and screened. We found that ZFN-injected fish breed normally and give clutches of similar size as when we intercross our non-ZFN injected wild-type stocks. Eggs from ZFN-injected females were fertilized in vitro with sperm from a male heterozygous for the *ntl*^{b195} allele. Of 7 females analyzed, 4 generated *ntl* progeny (Table 3; Fig. 4B) at frequencies ranging between 1–13% as gauged by this complementation cross (Table 3). To measure the frequency of gametes carrying gene disruptions, we directly genotyped the chromatid provided to the progeny (both wild-type and *ntl*) by four of the founder mothers, and found that the germline carried mutations at frequencies ranging from 5–32% (Table 3). Direct sequencing confirmed these estimates and revealed that three founders carried at least two new alleles, and one founder carried at least one (Fig. 4C). In addition to founders identified using complementation crosses and chromatid genotyping (Table 3), we have identified an additional 2 carriers (germline transmission rates of 33% and 53%) using complementation crosses and an additional 5 carriers (germline transmission rates of 6–25%) by analyzing haploids generated from founder females. Taken together, the data show that over 60% of *ntl* ZFN-injected founders (11/18) carry mutations at the *ntl* locus, with an average germline frequency of 20%.

To determine the level of specificity of ZFN function, an experimentally determined DNA binding consensus was derived for each ZFN (see Materials and Methods, Supplementary Fig. 11 online for experimental details). This information was then used to search the zebrafish genome for sites showing the highest similarity to their intended target site (Supplementary Fig. 11 online). To experimentally determine whether ZFNs cleave at these alternative “off-target” sites, we directly analyzed the top 5 potential off-target loci for each *ntl*-targeting ZFN pair. We used PCR to amplify the cognate chromosomal loci from phenotypically *ntl* progeny embryos (Table 3) carrying ZFN-induced mutations at the *ntl* gene, and analyzed them by direct sequencing, loss-of-RFLP, and mismatch endonuclease assays. All the chromatids we analyzed were wild-type (Supplementary Fig. 11 online). These results confirm that ZFNs can be used to specifically and efficiently create heritable mutant alleles at loci of interest.

Finally, to show that ZFN-induced alleles can be propagated in subsequent generations, we outcrossed two *ntl* ZFN-injected females (Females C and D, Table 3) and recovered heterozygous carrier individuals at frequencies consistent with the germline frequency of the mutation in each founder female (Table 3), indicating that heterozygosity for the new induced alleles was completely viable. As stocks reached sexual maturity, fish were intercrossed to siblings and backcrossed to founders. We recovered *ntl* mutant phenotypes in the expected ratios and observed no non-*ntl* phenotypes among F2 progeny. While our analysis has failed to reveal ZFN-induced mutations at loci other than *ntl*, in the hypothetical possibility that an undesired secondary mutation was occurring at a rate as high as 10%, it would rapidly segregate from the desired *ntl* mutation even after one generation.

Our data show ZFNs to be highly effective tools for inducing mutations at a specified locus in the zebrafish, the rapid production of embryos and adult animals with corresponding loss-of-function phenotypes (Tables 1 and 2) and adults carrying new alleles (Table 3). To serve this purpose, ZFNs can be injected as mRNA, thus allowing only transient nuclease expression, which we have shown to be sufficient to introduce a stable genetic mark on the targeted locus. The experiments in the present work describe the successful disruption of 3 distinct positions at 2 separate genetic loci and the use of ZFN injection into wild-type embryos to yield phenotypes expected from a loss of targeted gene function (Table 2). In addition, we show that ZFNs can be used to generate novel germline mutations with high specificity of action (Table 3; Supplementary Fig. 11 online).

The C₂H₂ zinc finger motif 19 has been engineered to recognize many distinct DNA sequences 14,20,21 (see also Supplementary Information online), and this has paved the way for the design of ZFNs used in efficient genome editing at a broad range of investigator-specified endogenous loci, including a mutation hotspot in a human monogenic disease locus 18. As our data show, the combination of this versatile platform with a rapid yeast-based assay for the identification of maximally active engineered ZFNs, open fundamentally novel avenues of experimentation in the zebrafish, and suggest that ZFN technology may be widely applied to many organisms for which reverse genetics strategies are currently unavailable.

MATERIALS AND METHODS

ZFN constructs

Detailed information, including full ZFN sequences, expression vector nomenclature, and a description of the design, assembly, and validation process, is provided in Supplementary information. Zinc finger proteins against zebrafish *gol* and *ntl* were designed and validated biochemically *in vitro* as described previously 18, 22, and cloned into expression vectors to generate zinc finger nucleases. In all experiments, the highfidelity, obligate-heterodimer 16 ZFN forms were used, except the experiments in Table 2 (also described in Supplementary Fig. 10 online), for which ZFNs carried wild-type FokI. In all other aspects, the nucleases had the same architecture as previously described 18. Note that requests for ZFN reagents other than those described here should be directed to zfn@sial.com, or via <http://www.sigma.com/zfn>.

Yeast assay

Detailed methods are provided in Supplementary Information. All strains were derived from the S288C parental strain 69-1B (*MATa*, *his3 200*, *lys2-128 δ* , *leu2 1*). The SSA reporter constructs were assembled into the *HO* targeting vector *HO*-poly-KanMX4-*HO* 23 by cloning two overlapping and non-functional fragments of the *MEL1* gene under the control of the *PGK1* promoter (Supplementary Fig. 3 online). ZFN were expressed using a galactose-inducible promoter 24, and inductions were performed as described 25 following the scheme presented in Fig. 1B. The quantitative α -galactosidase assay was performed as described with minor modifications 26.

Zebrafish mutant alleles, stocks, and husbandry

Zebrafish embryos were obtained by *in vitro* fertilization and natural spawnings of adults maintained at 28.5°C on a 14 h light, 10 h dark light cycle and staged as described 27. The *golden* (*gol^{b1}*) and *no tail* (*ntl^{b195}*) mutant alleles used have been previously described 12,28. The *ntl^{b487}* allele was identified in a forward genetic screen performed in Eugene, Oregon, and failed to complement two other *ntl* alleles (S.L. Amacher and C.B. Kimmel, unpublished data). Transheterozygotes were obtained in expected Mendelian ratios in at least two independent pairwise crosses (71/326 [22%] for *ntl^{b160}/ntl^{b487}* and 135/542 [25%] for *ntl^{b459}/ntl^{b487}*). Homozygous *ntl^{b487}* embryos have a less severe phenotype than that of the null allele, often having a more extensive, forked tail and patches of notochord tissue (Supplementary Fig. 7 online), in contrast to the complete lack of tail and notochord in null mutants 17.

Preparation and microinjection of ZFN mRNA

Matched *golden* ZFN pairs were subcloned into a pVAX vector with coding sequences separated by a 2A ribosome stuttering sequence for all experiments except those shown in Supplementary Fig. 10 online, which were done with separate expression constructs (see Supplementary Information online for vector maps, construct sequences, and recombinant DNA protocols and Supplementary Table 4 for plasmid names). In all cases, plasmids were linearized with Eag I and transcribed *in vitro* using the T7 mMessage mMachine transcription kit (Ambion, Austin, TX) to generate a single capped transcript containing both open reading frames. Approximately 5 nl of capped mRNA was injected into 1-cell zebrafish embryos at concentrations ranging from 0.04 ng/nl to 1 ng/nl.

Analysis of genome editing at ZFN target sites

A 312 bp region surrounding the *gol/slc24a5* Pair 14/15 cleavage site was amplified by PCR with primers 5'-ATCTGATATGGCCATGTCCAACATCG-3' and 5'-GGAACAATCCCATAACGCTCCTGCAG-3' and a 226 bp region surrounding the *ntl/Brachyury* Pair 2/3 cleavage site with primers 5'-ACGAATGTTTCCCGTGCTCAGAGCC-3' and 5'-GCTGAAAGATACGGGTGCTTTCATCCAGTGCG-3'. To analyze ZFN-induced mutations eliminating the BsrDI restriction site that lies between the left and right ZFN binding sites, PCR products were digested with BsrDI and resolved on a 2% agarose gel. BsrDI resistant sequences were 226 bp, while wild-type sequences were digested to 176 and 50 bp fragments. Heterozygous individuals carried all 3 band sizes. PCR products were ligated into the pCR[®] 4-TOPO[®] vector for sequencing (Invitrogen, Carlsbad CA).

For analysis of potential off-target action by the ZFNs, the position weight matrix (i.e., an experimentally determined consensus DNA binding site) for each ZFN was determined using an *in vitro* site selection method (Supplementary Information online). The off-target sites, and all the genotyping data, are provided in Supplementary Fig. 11 online.

Scoring of mosaic pigmentation in larval eyes

Two days after injection of *gol* ZFN mRNA, embryos were immobilized by immersion in 0.004% Tricaine and each eye was carefully evaluated for the appearance of small to large patches of unpigmented cells using an Olympus SZ60 dissecting microscope. Uninjected embryos had uniformly darkly pigmented eyes. Embryos were also scored for developmental defects.

In situ hybridization of *ntl* ZFN injected embryos

In order to analyze subtle notochord defects in *ntl* ZFN mRNA-injected embryos that may not have been detected by morphological analysis, embryos were sorted by phenotype and processed for *ntl* expression by whole mount *in situ* hybridization as previously described 29.

Imaging

Live and fixed embryos were mounted between bridged coverslips or in 3% methylcellulose and imaged on a Zeiss Axioplan 2 upright microscope. Digital images were taken with a Zeiss AxioCam camera.

Supplementary Material

Refer to Web version on PubMed Central for supplementary material.

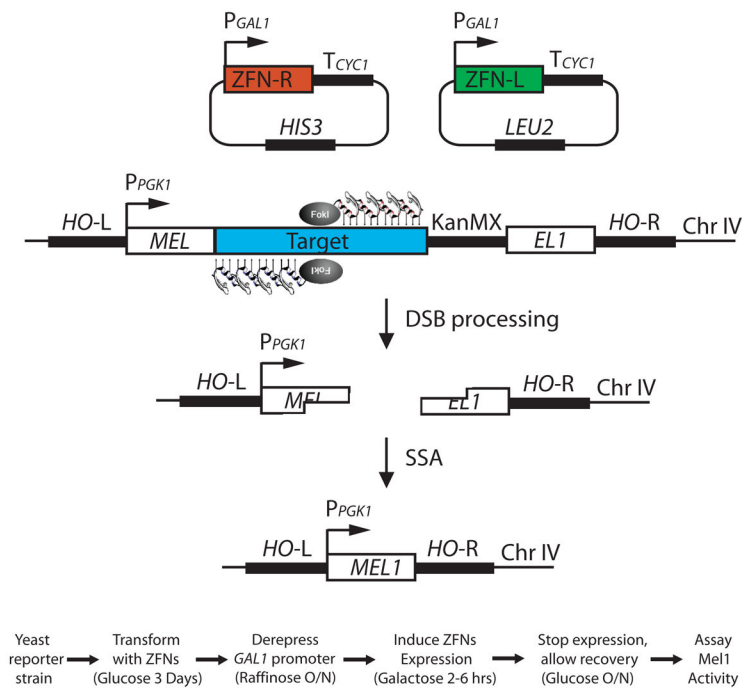
Acknowledgments

We thank Drs. Jasper Rine, Michael Holmes, Jacques Cote, and Amine Nourani for helpful suggestions regarding yeast-based screening of ZFNs, Drs. Randy Morse and Amine Nourani for providing reagents, Dr. Keith Cheng for *golden* cDNA, Drs. Keith Cheng and Herwig Baier for *golden* stocks, and Jennifer St. Hilaire, Emily Janus, and Kimberly Blum for excellent zebrafish care and technical support. We thank the anonymous referees for helpful suggestions on the manuscript. The *ntl^{b487}* allele was isolated in Eugene, OR in an NIH-funded screen (HD22486); S.L.A. gratefully acknowledges Dr. Charles Kimmel and our many colleagues at the University of Oregon who participated in mutagenesis screening. This work was supported by grants to S.L.A. from the NIH (1-R01-GM061952) and March of Dimes Birth Defects Foundation (1FY05-118). J.M.M. is supported by a National Science Foundation Predoctoral Fellowship.

References

1. Lieschke GJ, Currie PD. Animal models of human disease: zebrafish swim into view. *Nat Rev Genet.* 2007; 8:353–367. [PubMed: 17440532]
2. Nasevicius A, Ekker SC. Effective targeted gene ‘knockdown’ in zebrafish. *Nat Genet.* 2000; 26:216–220. [PubMed: 11017081]
3. Stemple DL. TILLING--a high-throughput harvest for functional genomics. *Nat Rev Genet.* 2004; 5:145–150. [PubMed: 14726927]
4. Thomas KR, Folger KR, Capecchi MR. High frequency targeting of genes to specific sites in the mammalian genome. *Cell.* 1986; 44:419–428. [PubMed: 3002636]
5. Sedivy, JM.; Joyner, AL. Gene targeting. Oxford University Press; Oxford: 1992.
6. Kim YG, Cha J, Chandrasegaran S. Hybrid restriction enzymes: zinc finger fusions to Fok I cleavage domain. *Proc Natl Acad Sci U S A.* 1996; 93:1156–1160. [PubMed: 8577732]
7. Smith J, Berg J, Chandrasegaran S. A detailed study of the substrate specificity of a chimeric restriction enzyme. *Nucleic Acids Res.* 1999; 27:674–681. [PubMed: 9862996]
8. Valerie K, Povirk LF. Regulation and mechanisms of mammalian double-strand break repair. *Oncogene.* 2003; 22:5792–5812. [PubMed: 12947387]

9. Bibikova M, Golic M, Golic KG, Carroll D. Targeted chromosomal cleavage and mutagenesis in *Drosophila* using zinc-finger nucleases. *Genetics*. 2002; 161:1169–1175. [PubMed: 12136019]
10. Morton J, Davis MW, Jorgensen EM, Carroll D. Induction and repair of zinc-finger nuclease-targeted double-strand breaks in *Caenorhabditis elegans* somatic cells. *Proc Natl Acad Sci U S A*. 2006; 103:16370–16375. [PubMed: 17060623]
11. Santiago Y, et al. Targeted gene knockout in mammalian cells using engineered zinc-finger nucleases. *Proc Natl Acad Sci U S A*. 2008; 105:5809–5814. [PubMed: 18359850]
12. Lamason RL, et al. SLC24A5, a putative cation exchanger, affects pigmentation in zebrafish and humans. *Science*. 2005; 310:1782–1786. [PubMed: 16357253]
13. Streisinger G, Coale F, Taggart C, Walker C, Grunwald DJ. Clonal origins of cells in the pigmented retina of the zebrafish eye. *Dev Biol*. 1989; 131:60–69. [PubMed: 2909409]
14. Pabo CO, Peisach E, Grant RA. Design and selection of novel Cys2His2 zinc finger proteins. *Annu Rev Biochem*. 2001; 70:313–340. [PubMed: 11395410]
15. Haber JE. In vivo biochemistry: physical monitoring of recombination induced by site-specific endonucleases. *Bioessays*. 1995; 17:609–620. [PubMed: 7646483]
16. Miller JC, et al. An improved zinc-finger nuclease architecture for highly specific genome editing. *Nat Biotechnol*. 2007; 25:778–785. [PubMed: 17603475]
17. Halpern ME, Ho RK, Walker C, Kimmel CB. Induction of muscle pioneers and floor plate is distinguished by the zebrafish *no tail* mutation. *Cell*. 1993; 75:99–111. [PubMed: 8402905]
18. Urnov FD, et al. Highly efficient endogenous human gene correction using designed zinc-finger nucleases. *Nature*. 2005; 435:646–651. [PubMed: 15806097]
19. Miller J, McLachlan AD, Klug A. Repetitive zinc-binding domains in the protein transcription factor IIIA from *Xenopus* oocytes. *Embo J*. 1985; 4:1609–1614. [PubMed: 4040853]
20. Pavletich NP, Pabo CO. Zinc finger-DNA recognition: crystal structure of a Zi268-DNA complex at 2.1 Å. *Science*. 1991; 252:809–817. [PubMed: 2028256]
21. Choo Y, Sanchez-Garcia I, Klug A. In vivo repression by a site-specific DNA-binding protein designed against an oncogenic sequence. *Nature*. 1994; 372:642–645. [PubMed: 7990954]
22. Zhang L, et al. Synthetic zinc finger transcription factor action at an endogenous chromosomal site. *J Biol Chem*. 2000; 275:33850–33860. [PubMed: 10913152]
23. Voth WP, Richards JD, Shaw JM, Stillman DJ. Yeast vectors for integration at the HO locus. *Nucleic Acids Res*. 2001; 29:E59. [PubMed: 11410682]
24. Mumberg D, Muller R, Funk M. Regulatable promoters of *Saccharomyces cerevisiae*: a comparison of transcriptional activity and their use for heterologous expression. *Nucleic Acids Res*. 1994; 22:5767–5768. [PubMed: 7838736]
25. Haber JE. Uses and abuses of HO endonuclease. *Methods Enzymol*. 2002; 350:141–164. [PubMed: 12073310]
26. Chen Q, et al. A yeast two-hybrid technology-based system for the discovery of PPARγ agonist and antagonist. *Analytical biochemistry*. 2004; 335:253–259. [PubMed: 15556564]
27. Kimmel CB, Ballard WW, Kimmel SR, Ullmann B, Schilling TF. Stages of embryonic development of the zebrafish. *Dev Dyn*. 1995; 203:253–310. [PubMed: 8589427]
28. Schulte-Merker S, van Eeden FJ, Halpern ME, Kimmel CB, Nüsslein-Volhard C. *no tail (ntl)* is the zebrafish homologue of the mouse T (Brachyury) gene. *Development*. 1994; 120:1009–1015. [PubMed: 7600949]
29. Jowett T. Analysis of protein and gene expression. *Methods Cell Biol*. 1999; 59:63–85. [PubMed: 9891356]



Strain	pGAL -HO	Galactose	
No target	-	-	
No target	-	+	
No target	+	-	
No target	+	+	
Synthetic HO site	-	-	
Synthetic HO site	-	+	
Synthetic HO site	+	-	
Synthetic HO site	+	+	

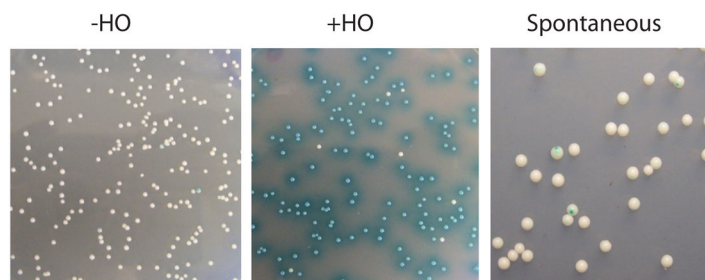


Figure 1. Yeast-based system of identification of maximally active ZFNs

(A) Components of yeast-based chromosomal reporter system: expression vectors for the ZFNs (top), target gene integrated into the chromosome at the HO locus (middle). After a double-strand break (DSB) is induced at the target by a pair of ZFNs, it is processed via single-strand annealing (SSA) to repair the *MEL1* reporter gene, the activity of which can be rapidly assayed in liquid culture. (B) Outline of procedure for ZFN activity measurement in yeast. (C) Reporter gene restoration is dependent on a precisely targeted DSB. A reporter gene was engineered as in Fig. 1A, except it carried a recognition site of the HO

endonuclease. MelI activity is only observed following induction of expression of the endonuclease (“+gal”), and of its target in the reporter locus (bottom row). (D) Exceedingly low frequency of spontaneous *MELI* gene repair. Essentially no MelI activity is observed when HO expression is not induced (left panel), with the exception of very low-frequency spontaneous *MELI* restoration events (right panel), visualized as small sectors of blue cells within otherwise white colonies. As shown in the middle, induction of HO endonuclease expression converts the overwhelming majority of the cells in the sample to a *MELI* state.

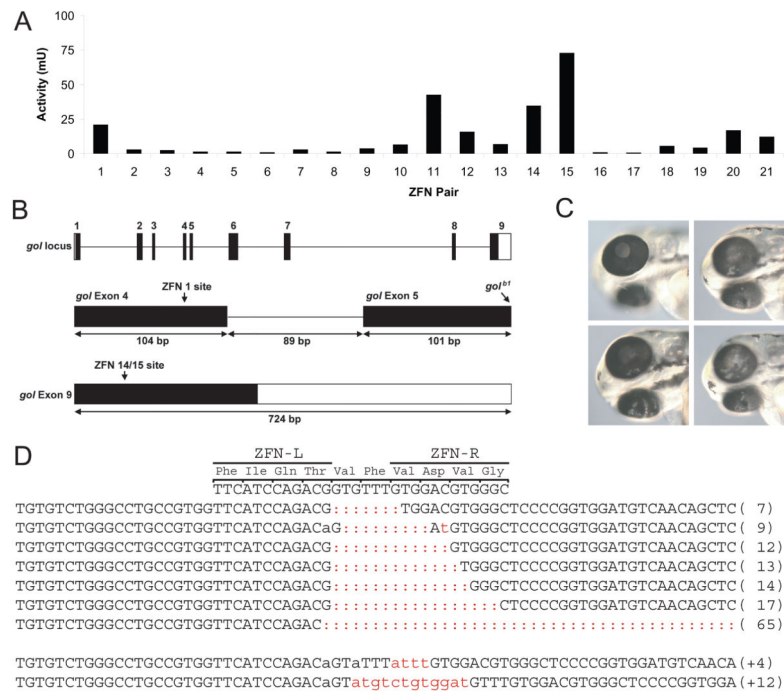


Figure 2. Injection of golden ZFN-encoding mRNA into zebrafish embryos induces targeted loss-of-function mutations in somatic cells

(A) Twenty one pairs of high-fidelity, obligate-heterodimer 16 ZFNs (Supplementary Table 1) targeting the *gol* locus were screened for activity in yeast using the assay shown in Fig. 1, with the exception that Mel1 activity was assayed in the yeast growth medium, rather than relying on the number of *MEL1*-positive colonies. For each ZFN pair, activity in the medium of the Mel1 enzyme is listed in mU, as detected after induction by galactose. (B) Schematic of the *gol* locus indicating recognition sites of three ZFN pairs chosen for further testing. ZFN pair 1 recognizes a site within Exon 4 upstream of the loss-of-function *gol*^{bl} allele, whereas ZFN pairs 14 and 15 both recognize a site within the last exon upstream of coding sequence for two putative C-terminal transmembrane helices. (C) Injection of ZFN pair 14 mRNA (5 ng) into *gol*^{bl} heterozygous 1-cell embryos induces somatic loss-of-function mutations in the wild-type *gol* allele. The 2 dpf embryo on the top left shows no evidence of loss of heterozygosity; the eyes are uniformly and darkly pigmented like wild-type embryos. Single or multiple patches of unpigmented cells can be observed in *gol* ZFN-injected embryos (remaining three panels), and sometimes mosaic patches were seen in both eyes. Except for these pigment clones, the embryos shown were phenotypically normal. (D) When PCR products from pooled individuals were sequenced, deletions and insertions typical of NHEJ were observed. In some cases, these are in frame and in other cases are frameshifts.

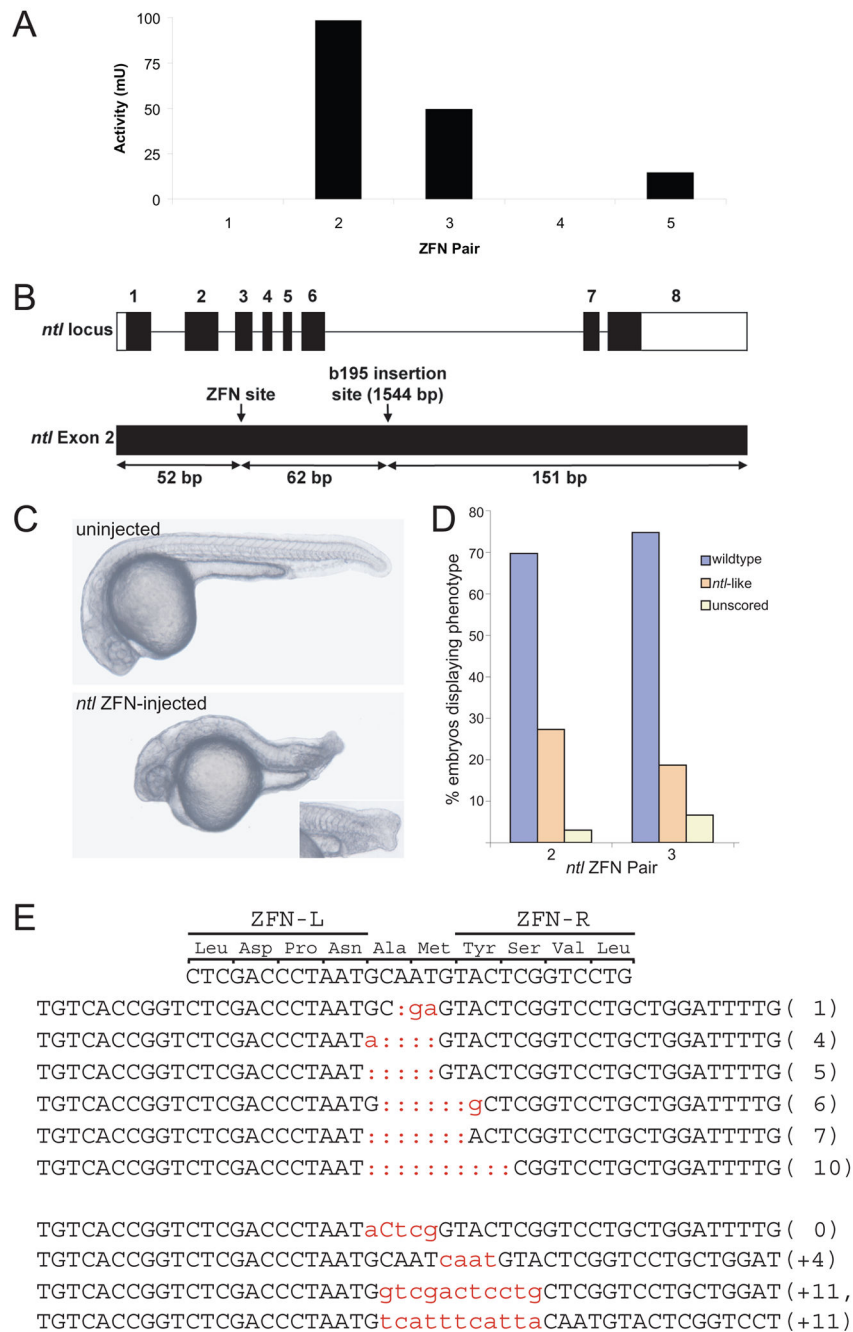


Figure 3. Injection of *no tail* ZFN-encoding mRNA into zebrafish embryos induces targeted loss-of-function mutations in somatic cells

(A) Five high-fidelity, obligate-heterodimer 16 ZFN pairs (Supplementary Table 2) targeting the *ntl* locus were screened for activity using the yeast-based assay shown in Fig. 1. See Fig. 2A legend for details. (B) Schematic of the *ntl* locus indicating the recognition site of the ZFN pairs chosen for further testing. ZFN pairs 2 and 3 recognize the same site within Exon 2 just upstream of the site of the loss-of-function *ntl*^{b195} insertion allele. (C) Injection of 5 ng *ntl* ZFN pair 2 mRNA into 1-cell *ntl*^{b195} heterozygous embryos induces mutations in the

wild-type *ntl* allele. Compared to uninjected embryos at 1 dpf (top panel), ZFN-injected embryos lack a notochord and tail like null mutants, or have patchy notochords and forked tails (inset), like hypomorphic *ntl* mutants. (D) Graph showing the percentage of *ntl*^{b195} heterozygous embryos displaying wild-type or *ntl* mutant phenotypes after injection of 5 ng mRNA encoding either ZFN pair 2 or ZFN pair 3. A small percentage of injected embryos were defective (“unscored”). Approximately one-quarter of the *ntl*-like embryos were slightly more necrotic than the typical *ntl* mutant (4/17 for ZFN pair 2 and 5/18 for ZFN pair 3). (E) When PCR products from pooled *ntl*-like individuals were sequenced, deletions and insertions typical of NHEJ were observed. In some cases, these are in frame and in other cases cause frameshifts.

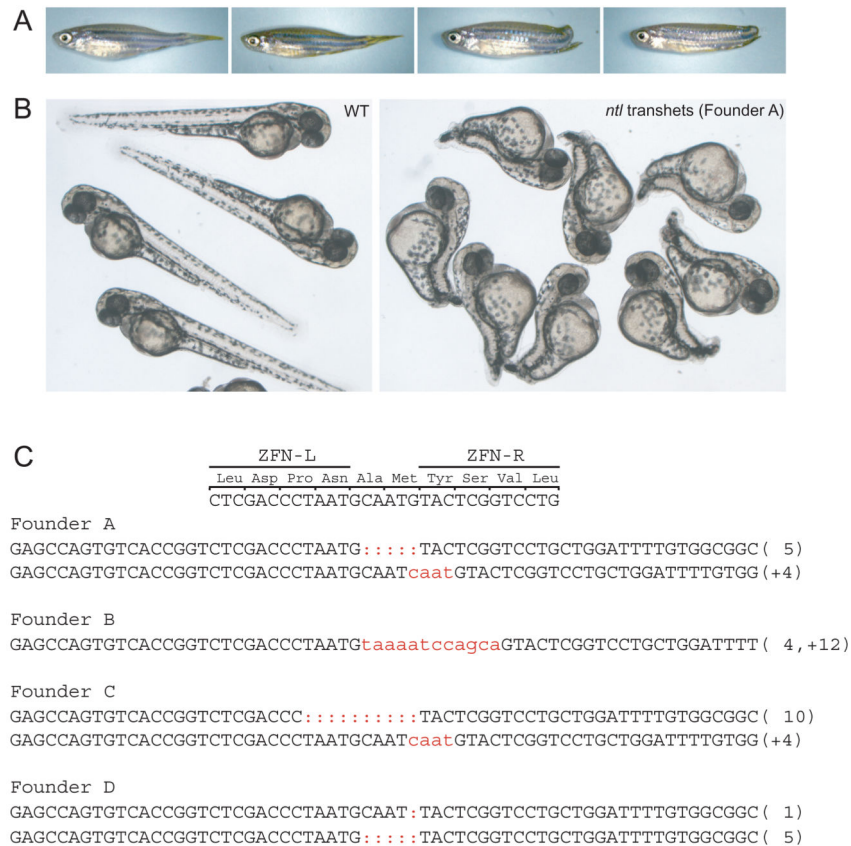


Figure 4. Injection of *no tail* ZFN-encoding mRNA in wild-type embryos creates novel *ntl* mutations that are transmitted through the germline

(A) Some juvenile fish derived from wild-type embryos injected with mRNA encoding *ntl*-targeting ZFNs (both conventional and high-fidelity FokI domains, the latter shown here) show posterior truncations. Right two panels show posteriorly truncated juveniles; left panels are normal-appearing siblings. (B) *ntl* phenotypes observed in progeny of ZFN-injected founder animals in complementation crosses at 2 dpf. Wild-type embryos injected with mRNA encoding high-fidelity, *ntl*-targeting ZFNs were grown to adulthood and eggs from founder females were fertilized in vitro with sperm from a *ntl*^{b195} heterozygous male. Representative progeny from this complementation test with Founder female A are shown in the right panel. (C) Novel *ntl* alleles (7 total) carried by founders that gave phenotypically *ntl* progeny in complementation cross (see also Table 3). Founder A was derived from a wild-type embryo injected with ZFN pair 2 (5 ng mRNA), and founders B through D from wild-type embryos injected with ZFN pair 3 (5 ng mRNA).

TABLE 1

ZFNs directed to the zebrafish *golden* gene induce somatic loss-of-function phenotypes.

ZFN pair ¹	Dose (ng)	Normal embryos		Abnormal embryos ²			Total WT eye pign	Total <i>gol</i> clones
		WT eye pigment	<i>gol</i> eye clones	WT eye pigment	<i>gol</i> eye clones	Not scored		
14	0.2	54/58 (93%)	1/58 (2%)	2/58 (3%)	0/58 (0%)	1/58 (2%)	56/58 96%	1/58 2%
	1.0	39/42 (93%)	2/42 (5%)	0/42 (0%)	1/42 (2%)	0/42 (0%)	39/42 93%	3/42 7%
	5.0	26/49 (53%)	11/49 (22%)	0/49 (0%)	5/49 (10%)	7/49 (14%)	26/49 53%	16/49 32%
15	0.2	42/45 (93%)	1/45 (2%)	0/45 (0%)	0/45 (0%)	2/45 (4%)	42/45 93%	1/45 2%
	1.0	26/29 (90%)	3/29 (10%)	0/29 (0%)	0/29 (0%)	0/29 (0%)	26/29 90%	3/29 10%
	5.0	24/37 (65%)	9/37 (24%)	0/37 (0%)	3/37 (8%)	1/37 (3%)	24/37 65%	12/37 32%
1	0.2	11/11 (100%)	0/11 (0%)	0/11 (0%)	0/11 (0%)	0/11 (0%)	11/11 100%	0/11 0%
	1.0	48/50 (96%)	0/50 (0%)	0/50 (0%)	0/50 (0%)	2/50 (4%)	48/50 96%	0/50 0%
	5.0	45/70 (64%)	7/70 (10%)	9/70 (13%)	2/70 (3%)	7/70 (10%)	54/70 77%	9/70 13%
	7.0	78/123 (63%)	26/123 (21%)	12/123 (10%)	3/123 (2%)	4/123 (3%)	90/123 73%	29/123 24%

¹ High-fidelity, *gol*-targeting ZFN mRNA was injected into 1-cell embryos heterozygous for the *gol^{b1}* allele at the indicated dose. Eye pigmentation mosaicism was scored at 48 hpf and embryos having at least one clone of unpigmented cells in an otherwise dark eye were scored as having *gol* eye clones. Representative examples are shown in Fig. 2C.

² Most embryos in this category had slight to moderate developmental defects. Common syndromes were a bent body axis or slight head necrosis. The embryos in the "Not scored" column had severe developmental defects that precluded scoring of eye pigmentation mosaicism.

ZFNs directed to the zebrafish *no tail* gene induce loss-of-function mutations on both chromatids early in development

TABLE 2

<i>ntl</i> ZFN pair ¹	Dose (ng)	Embryos injected	Live embryos at 24h	Scoreable embryos at 24h	WT phenotype	<i>ntl</i> phenotype	WT ISH phenotype	<i>ntl</i> ISH phenotype
2	0.2 each	100	94/100 (94%)	88/100 (88%)	68/88 (77%)	20/88 ² (23%)	N.D.	N.D.
	1.0 each	101	87/101 (86%)	60/101 (59%)	17/60 (28%)	43/60 ³ (72%)	N.D.	N.D.
	6.0 each	120	39/120 (33%)	24/120 (20%)	4/24 (17%)	20/24 ⁴ (83%)	3/17 (17%)	14/17 (83%)

¹The ZFN pairs contained wild-type, rather than high-fidelity 16 FokI endonuclease domains, and were injected as mRNA into 1-cell wild-type zebrafish embryos.

²All of the 20 *ntl*-like embryos had a hypomorphic *ntl*^{b487} phenotype.

³13/43 (30%) had a null *ntl* phenotype, the remaining 70% had hypomorphic phenotypes.

⁴Virtually all embryos had a null *ntl* phenotype; approximately half were more necrotic than usual (see also Supplementary Fig. 10 online).

ZFNs directed to the zebrafish *no tail* gene induce loss-of-function germline mutations

TABLE 3

Founder	Complementation testing data			Chromatid genotyping data ² (Frequency of <i>ntl</i> allele disruption)				
	WT progeny	<i>ntl</i> progeny	Unscored progeny ¹	% germline	WT progeny	<i>ntl</i> progeny	Unscored progeny	Total
A	109/118 92.4%	9/118 7.6%	0/118 0%	15.3%	11/96 11.5%	9/9 100%	N.A.	20/105 19%
B	77/82 93.9%	1/82 1.2%	4/82 4.9%	2.4%	1/77 1.3%	1/1 100%	2/4 50%	4/82 4.9%
C	37/50 74%	3/50 6%	10/50 20%	12%	9/37 24.3%	3/3 100%	3/7 42.9%	15/47 31.9%
D	12/15 80%	2/15 13.3%	1/15 6.4%	26.7%	2/12 16.7%	2/2 100%	0/1 0%	4/15 26.7%

¹These progeny could not be conclusively phenotyped.

²The ZFN target site overlaps a BsrDI restriction site. The chromatids were genotyped by amplifying the ZFN targeted stretch by PCR using primers that do not amplify the *ntl*^{b195} allele, and measuring the frequency of disrupted alleles by determining the fraction of BsrDI-resistant PCR products.